



Self-consistent description of the core and boundary plasma in the high-field ignition experiment

R. Stankiewicz, R. Zagórski *

Institute of Plasma Physics and Laser Microfusion, 23 Hery Street, P.O. Box 49, 00-908 Warsaw, Poland

Abstract

A model has been developed which is capable to describe in a self-consistent way plasma dynamics in the center and edge regions of fusion reactor. The core plasma is treated in the frame of 1-D radial transport model whereas a 1-D analytical model along magnetic field lines for plasma and impurity transport outside the last closed magnetic surface (LCMS) is applied. The model is suitable to fast scans of the parameter space of the tokamak type reactor and has been used to investigate operation regimes of the high-field IGNITOR experiment. © 2001 Elsevier Science B.V. All rights reserved.

Keywords: Tokamak; Edge modelling; Computer simulation

1. Introduction

In recent years the necessity of the self-consistent modelling of the plasma dynamics in the core and the scrape-off layer (SOL) has been widely recognized. Various efforts have been made in the development of global transport codes [1,2]. Due to the complexity of the problem and different topologies of magnetic field lines and time scales in both regions some numerical problems appear. The attempt to model all the physical details results in huge computer programs requiring a large amount of computer time. In the paper a simple self-consistent model for the core and the SOL is presented, which is able to describe the plasma and impurity behaviour in the inner wall configuration of the IGNITOR experiment [3]. The model has been used to analyze the influence of the core-SOL coupling due to the production of sputtered impurities and its cooling effect on the reactor parameters. The problem of the choice of suitable materials for the plasma facing components in the high field fusion reactor is also addressed. Calculations have been performed to investigate oper-

ating regimes of the IGNITOR experiment with different first wall materials (C, Ni). Results show that it is possible to achieve ignition condition in the compact, ohmically heated tokamak.

2. Physical model

The model consists of 1-D analytical model for SOL plasma and 1-D core radial transport model for heat, bulk ions and impurities. The energy losses due to Bremsstrahlung and line radiation of sputtered and injected impurities as well as alpha particles heating are included into the model.

2.1. Background plasma

The plasma temperatures in the core (T_e, T_i) are determined by solution of the conductivity equations. The energy sources are due to the Ohmic heating (P_{OH}) and the alpha particles heating (P_α) whereas losses are caused by Bremsstrahlung (P_B) and line radiation (P_{lin}).

$$\frac{3}{2}n_e \frac{\partial T_e}{\partial t} + \frac{1}{r} \frac{\partial}{\partial r} \left(m_e \chi_e \frac{\partial T_e}{\partial r} \right) = P_{OH} + P_\alpha - P_B - P_{lin} - Q_{ei}, \quad (1)$$

* Corresponding author. Tel.: +48-22 666 8372; fax: +22-666 83 72.

E-mail address: zagorski@ifpilm.waw.pl (R. Zagórski).

$$\frac{3}{2} n_i \frac{\partial T_i}{\partial t} - \frac{1}{r} \frac{\partial}{\partial r} \left(r n_i \chi_i \frac{\partial T_e}{\partial r} \right) = Q_{ei}, \quad (2)$$

where Q_{ei} is the energy equilibration term, $\chi_{e,i}$ the heat conduction coefficient for electrons and ions, respectively and $n_{e,i}$ is the electron (ion) density. The energy losses due to the Bremsstrahlung and the line radiation are calculated using the impurities distribution obtained by solving the impurity transport model. Since no reliable, theory based, transport models exist at present, we are using local transport models that reproduce the global confinement predictions for the tokamak reactor [4]: $\chi_{e,i} = C_{e,i}(1 + r^2/a^2)a^2/\tau_E$, where $C_e = 2C_i$ is an adjustable coefficients. The energy confinement time τ_E is defined by the ITER96 scaling law [5]

$$\tau_E = 0.023 I_p^{0.96} B_T^{0.03} P_{\text{tot}}^{-0.73} \bar{A}_i^{0.2} R_T^{2.1} \kappa^{0.64} a^{-0.06} R_T^{1.89} \bar{n}_e^{0.4} \quad (3)$$

(with the units s, MA, T, MW, m and 10^{19} m^{-3}), where I_p is the total plasma current, κ the elongation of the plasma cross-section, R_T the toroidal radius, a is the plasma radius, \bar{A}_i the mean ion mass number, B_T the toroidal magnetic field and \bar{n}_e is the line average density. The value of $C_e = 0.25$ was chosen to get the agreement between the energy confinement time calculated from the scaling law (Eq. (3)) and obtained from the code. It should be noted that our heat transport model cannot describe the transport barrier. However, for IGNITOR, the existence of such barrier has not been demonstrated theoretically even for very sophisticated transport models [3,5] as well as the experimental results for the high density limiter tokamak e.g., FTU does not exhibit the transport barrier.

The background ions are described by the diffusion equation.

$$\frac{\partial n_i}{\partial t} - \frac{1}{r} \frac{\partial}{\partial r} \left[r \left(D_i^{\text{an}} \frac{\partial n_i}{\partial r} - n_i V_i^{\text{pinch}} \right) \right] = S_i, \quad (4)$$

where $V_i^{\text{pinch}} = -2D_i^{\text{an}}r/a^2$ is the pinch velocity and the diffusion coefficient and the source are chosen in the form $D_i^{\text{an}} = C_D \chi_e$ (C_D – an adjustable parameter) and $S_i = S_{i0}(1 - (r/a)^2)^4$, respectively. The assumed profile of the particle source leads to parabolic-like profile of the ion density as achieved in the recent calculations of the IGNITOR parameters [5]. The electron density is defined by the neutrality condition and the value of S_{i0} is determined by the condition that the averaged electron density is prescribed.

In the present model we assume that the profile of plasma current (j_ϕ) is described with a generalized parabola: $j_\phi(r) = j_{\phi 0}(1 - (r/a)^2)^{1.5}$.

2.2. Modelling of impurity transport

In our model we allow for two types of impurities: seeded impurities n_z^{inj} and intrinsic impurities n_j ($n_z^{\text{tot}} = n_z^{\text{inj}} + \sum_j n_j$). For the sputtered impurities we apply 1-D radial transport model. In order to simplify the calculations we assume the fixed profile of the injected impurity given by [2]: $n_z^{\text{inj}} = (n_e/n_{es})^{\alpha_z} n_{zs}^{\text{inj}}$ with the peaking factor $\alpha_z = 0.5$ consistent with a flat Z_{eff} radial profile [4] ($n_{es}, (n_{zs}^{\text{inj}})$ – electron (impurity) density at the last closed magnetic surface (LCMS)). The assumed profile of the impurity is the same as in simulations of high field FTU tokamak [6] leading to reasonable agreement with experiment. The injected impurity cooling rate is calculated assuming corona equilibrium [7].

In order to consider different charge states of intrinsic impurity ions (n_j), generated by sputtering processes at the limiter plates, and their energy losses in the bulk plasma the multifluid radial transport of impurity ions has been used: [4,8]

$$\frac{\partial n_j}{\partial t} + \frac{1}{r} \frac{\partial}{\partial r} (r \Gamma_j) = n_{j-1} \alpha_{j-1} - n_j (\alpha_j + \beta_j) + n_{j+1} \beta_{j+1} \\ j = 1, \dots, Z_{\text{max}}. \quad (5)$$

where Z_{max} is the sputtered impurity atomic number, n_j the impurity ion density in the j th ionization state, α_j the ionization rate coefficient and β_j is the total (radiative and dielectronic) recombination rate coefficient [8]. The flux of impurity ions in the j th ionization state is given by [4,8]: $\Gamma_j = \Gamma_j^{\text{nc}} + \Gamma_j^{\text{an}}$, where Γ_j^{nc} is the neoclassical flux and Γ_j^{an} is the anomalous flux. For Γ_j^{nc} we have taken the formula of Rutherford [9] in test particle approximation with the adjoint of the classical term

$$\Gamma_j^{\text{nc}} = (1 + q_c) \frac{\rho_p^2 v_{\rho i}}{Z_j T_i} \left[T_i \frac{\partial n_i}{\partial r} - \frac{n_i}{Z_j n_j} T_j \frac{\partial n_j}{\partial r} - \frac{n_i}{Z_j} \frac{\partial T_j}{\partial r} \right], \quad (6)$$

where $v_{\rho i}$ is the collision frequency between ions and deuterons (tritons), q_c the safety factor, ρ_p the Larmor radius for deuterons (tritons) and Z_j is the ion charge in the j th ionization state. It is assumed that all ions have the same temperature $T_i = T_j$.

The anomalous flux Γ_j^{an} is given by: $\Gamma_j^{\text{an}} = -D_j^{\text{an}} \partial n_j / \partial r + n_j V_j^{\text{pinch}}$, where the anomalous pinch velocity V_j^{pinch} has the form: $V_j^{\text{pinch}} = -2\gamma_D D_j^{\text{an}} r/a^2$ with $D_j^{\text{an}} = 1 \text{ m}^2/\text{s}$ and $\gamma_D (= 0.1)$ being an adjustable coefficient.

The impurity density at LCMS n_{zs}^{sput} calculated from the SOL model, determines the boundary conditions for the impurity transport equations: $n_j(a) = n_{js}$. For simplicity it is assumed that impurity ions at the boundary are distributed according to the corona equilibrium. The electron density n_e is calculated from the quasi-neutrality condition $n_e(r) = n_i(r) + 2n_{\text{He}}(r) + Z(r)n_z^{\text{inj}}(r) + \sum_j Z_j n_j$, where n_{He} is the helium density. Due to low concentration of alpha particles (0.05%)

expected in IGNITOR [3,5] the impact of alpha particles on the results of calculations is not very important, and the alpha particle density proportional to ions density has been assumed for simplicity.

2.3. SOL plasma

In the boundary plasma, background ions are described by the two-point model taking into account the gradients of plasma parameters in the SOL [10]. We solve the continuity, momentum and energy equations along field lines. Equal ions and electron temperatures are assumed and the uniform sources of particles and energy from the plasma core. The equations are integrated from the stagnation point to the target plate by using standard sheath conditions as boundary conditions at limiter plates [11].

The condition for the temperature at the target plate can be written as

$$P_{\text{plate}}(T_p) \equiv \left[\delta_i (\Gamma_{\text{ip}} + \Gamma_{\text{zp}}^{\text{sput}}) + \delta_e \Gamma_{\text{ep}} \right] T_p \\ = P_{\text{inp}}(T_p) - P_{\text{rad}}^{\text{SOL}}(T_p), \quad (7)$$

where the power entering SOL is given by $P_{\text{inp}} = P_{\text{OH}} + P_{\alpha} - P_{\text{B}} - P_{\text{lin}}$, δ_i , δ_e are the energy transmission factors [11], $\Gamma_{\text{ip}} = n_{\text{ip}} c_s S_{\text{eff}}$, $\Gamma_{\text{ep}} = n_{\text{ep}} c_s S_{\text{eff}}$ are the main ions and electrons fluxes to the plate, respectively, and $\Gamma_{\text{zp}}^{\text{sput}} = n_{\text{zp}}^{\text{sput}} c_s M_{\text{zp}}^{\text{sput}} S_{\text{eff}}$ is the sputtered impurity ions flux to the plate. $M_{\text{zp}}^{\text{sput}}$ is the sputtered impurity Mach number, c_s the sound speed and S_{eff} is the effective area of the limiter plates. The plasma density at the plate for a given input (to the SOL) particle flux Γ_{inp} and recycling coefficient $R \equiv 1 - \Gamma_{\text{inp}}/\Gamma_{\text{ip}}$ can be evaluated as: $n_{\text{ip}} = \Gamma_{\text{inp}}/S_{\text{eff}}/(1-R)/c_s$, where the recycling coefficient $R = 0.9$ is an input variable in these simulations. The upstream plasma temperature T_s and density n_{es} can be expressed by the plasma parameters at the plate [10]

$$T_s = T_p \left[1 - \frac{7}{2} \frac{P_{\text{inp}}}{\lambda_0 T_s^{7/2} V^{\text{SOL}} L_c^2} \right]^{-1} \quad n_{\text{es}} T_s = 2n_{\text{ep}} T_p, \quad (8)$$

where $\lambda_0 = 1.5/Z_{\text{eff}} \times 10^{22} \text{ eV}^{-5/2} \text{ m}^{-1}$ is the heat conduction coefficient, $V^{\text{SOL}} \equiv S_{\text{eff}} L_c$ is the SOL volume, L_c is the distance from stagnation point to the plate.

As regard the impurity transport we should distinguish between seeded and intrinsic impurity. It is assumed for the sake of simplicity that the concentration of injected impurity is constant in the SOL: $n_{\text{zs}}^{\text{inj}} = n_{\text{zp}}^{\text{inj}} = n_z^{\text{inj}}(a)$. The assumption of the uniform distribution of the injected impurity in the SOL may slightly underestimate the radiation in the SOL and simplifies the role of injected impurity in the SOL.

The intrinsic impurity ion flux at the plate $\Gamma_{\text{zp}}^{\text{sput}}$ is determined by the stationary condition $\Gamma_{\text{op}} = \Gamma_{\text{zp}}^{\text{sput}}$, where Γ_{op} is the impurity atoms flux from the plate given

by: $\Gamma_{\text{op}} = Y_{\text{H}} \Gamma_{\text{ip}} + Y_z \Gamma_{\text{zp}}^{\text{sput}}$ with Y_{H} , Y_z being sputtering and self-sputtering yields averaged over the scrape-off layer width. Now, assuming that the impurity plate velocity equals to $V_{\text{zp}} = M_{\text{zp}}^{\text{sput}} c_s$ the expression for the impurity plate density can be found: $n_{\text{zp}}^{\text{sput}} = Y_{\text{eff}} n_{\text{ip}}/M_{\text{zp}}^{\text{sput}}$ where Y_{eff} is the effective sputtering yield defined as $Y_{\text{eff}} = Y_{\text{H}}/(1 - Y_z)$. In order to close the self-consistent description of the reactor plasma it is necessary to determine the impurity density at the LCMS $n_{\text{zs}}^{\text{sput}}$, which depends in the limiter tokamak mainly on the transport properties of the impurity ions in the SOL. The density of the intrinsic impurity at the LCMS is prescribed in terms of so-called retention factor in the present model: $n_{\text{zs}} = \mathcal{A}_{\text{sol}} n_{\text{zp}}^{\text{sput}}$ where \mathcal{A}_{sol} is evaluated in Ref. [12] on the basis of 1-D transport model.

Radiation of impurity ions in the SOL is proportional to the impurity density at the separatrix and SOL volume. In the model impurities generated at the plate due to sputtering processes and impurities injected to the plasma give rise to the SOL radiation. Also hydrogen radiation is included in the model: $P_{\text{rad}}^{\text{SOL}} = R \Gamma_{\text{inp}} E_{\text{H}} / (1 - R) + V^{\text{SOL}} n_{\text{es}} (n_{\text{zs}}^{\text{sput}} L_z^{\text{sput}} + n_{\text{zs}}^{\text{inj}} L_z^{\text{inj}})$, where E_{H} is the average energy loss per ionization event for hydrogen ($E_{\text{H}} = 17.5 \text{ eV}$). The cooling rates L_z^{sput} , L_z^{inj} are calculated for the sake of simplicity from the corona equilibrium, therefore it is expected to be slightly underestimated.

3. Results and discussion

We have simulated stationary operating regimes of the IGNITOR tokamak for two characteristic wall materials (C, Ni). An IGNITOR [3,5] reference case ($R_T = 1.32 \text{ m}$, $a = 0.47 \text{ m}$, $I_p = 12 \text{ MA}$, $0.054\% \text{ He}$) is assumed. The energy confinement time calculated in the code with the prescribed value of the diffusion coefficient ($C_e = 0.25$) varies from 0.3 to 0.6 s in agreement with the project prediction. It has been found that for the large range of the average electron density $\langle n_e \rangle (3 \times 10^{20} - 8 \times 10^{20} \text{ m}^{-3})$ the solution with burning plasma exists for relatively low plasma temperature in the center $T_e(0)$ (10–16 keV). Simultaneously the ohmic heating is significant and remains comparable with the alpha heating power for small values of $\langle n_e \rangle$.

It can be seen that the influence of the sputtered impurities on the overall energy balance depends strongly on the coupling between the core and SOL region. The coupling between the core and SOL region can be modified in the simulation by changing the ion diffusion. The results are presented in Figs. 1 and 2 for both Ni and C limiter plates. It should be noted that for the Ni plates the coupling with the SOL manifests itself by the strong line radiation due to sputtered Ni ions. For the C plate the sputtered C ions increase the dilution of

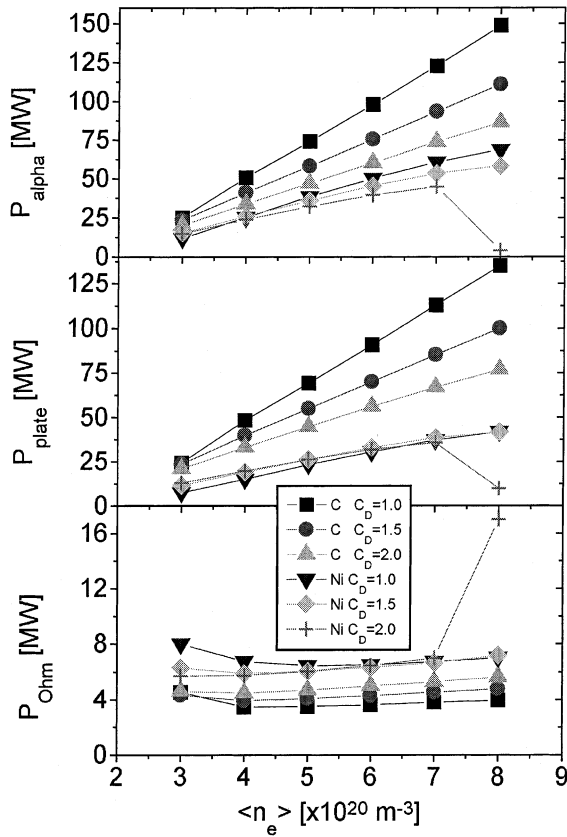


Fig. 1. P_α , P_{plate} , P_{ohm} , versus average electron density $\langle n_e \rangle$ for carbon and nickel plates.

the core plasma, whereas line radiation is small. The difference between both materials can be clearly seen in the figures (Figs. 1 and 2). Nevertheless the general tendencies are the same. The alpha power (P_α), the power losses relative to total power (P_{loss}) and the effective charge decrease with the increase of the radial transport of the bulk ions. This effect can be explained by the increase of the screening efficiency of the SOL with the increase of the particle flux to the SOL. For the nickel plates the influence of the core-SOL coupling on the energy losses and the effective charge is stronger. On contrary the alpha power is more strongly modified by the SOL-core coupling for C plate. It should be noted that the power flowing to the plate is much lower for the Ni plate than for C plate and it is practically the same for all considered values of the diffusion coefficients. The increase of the alpha power in the case of the Ni plate is compensated by the increase of the impurity radiation and simultaneously, the plasma contamination is low and Z_{eff} remains relatively small almost for all considered plasma densities. The screening efficiency of the SOL is responsible also for the behaviour of the alpha power, the effective charge and the power losses with

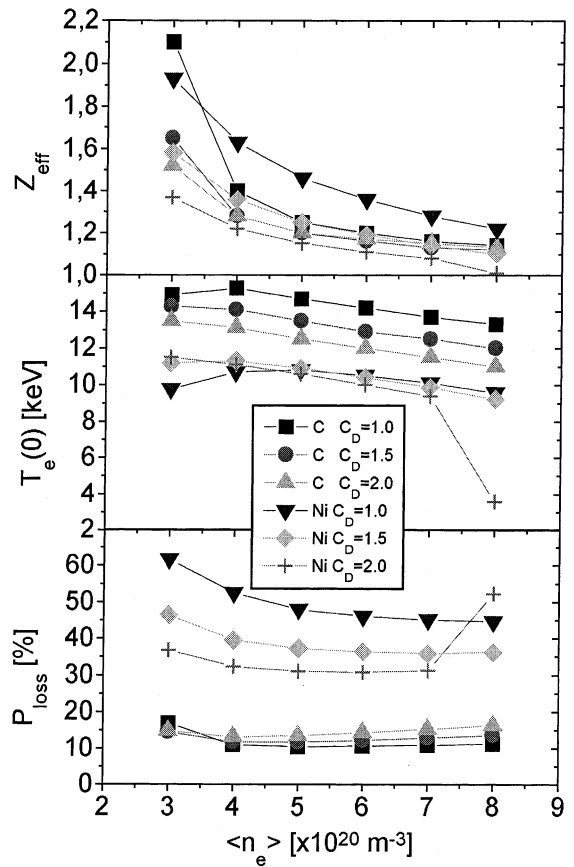


Fig. 2. Z_{eff} , $T_e(0)$ and P_{loss} versus average electron density $\langle n_e \rangle$ for carbon and nickel plates.

respect to the averaged plasma density $\langle n_e \rangle$. The particle flux flowing to the SOL depends on the averaged plasma density and is lower for low plasma density. The lower particle flux to the SOL corresponds to lower screening efficiency of the SOL and the increase of the impurity concentration. This explains the increase of the relative energy loss P_{loss} and the effective charge Z_{eff} for small plasma densities. The presented results show only the general tendency connected with the SOL-core coupling. In order to assess more precisely the effect of the core-SOL coupling the ion diffusion model taking into account the physical mechanisms of the ion transport should be used. This problem will be considered in the future.

The possibility of the reduction of the power load to the C plate by injected impurity has been also investigated. The results of numerical simulation are presented in Figs. 3 and 4 for Argon as injected impurity (with $C_D = 1.5$). The overall behaviour of P_α , Z_{eff} and P_{loss} with respect to the concentration of Ar is similar as for the case of the sputtered impurity. The reduction of the power flowing to the plate and the core plasma

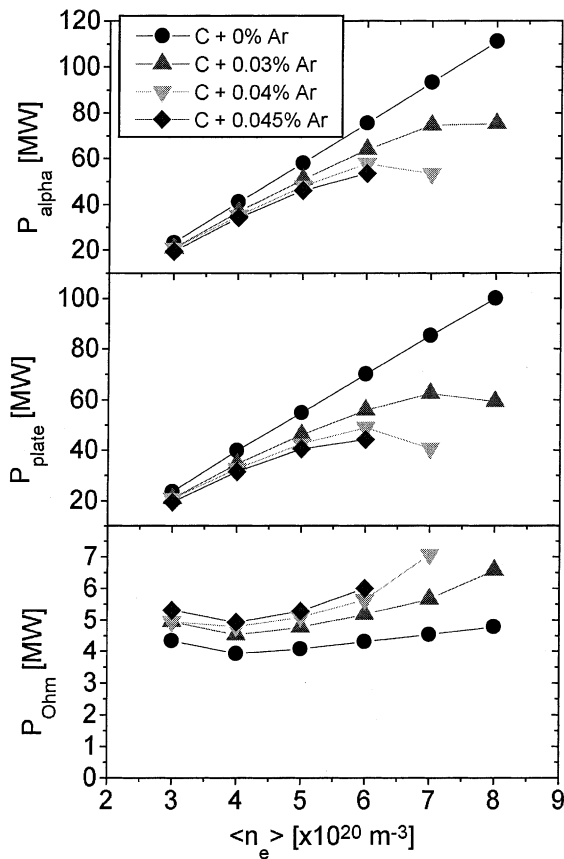


Fig. 3. P_α , P_{plate} , P_{ohm} , versus average electron density $\langle n_e \rangle$ for carbon plate with different concentrations of Ar.

temperature $T_e(0)$ can be observed. However, for higher concentration of the injected impurity the upper limit of the plasma averaged density $\langle n_e \rangle$ appears above which there is no stationary solution with burning plasma. The upper limit decreases with the injected impurities concentration. Similar limit has been found in the case of ITER like tokamak [10]. Consequently it is impossible to reduce the power load to the C plate with Argon as injected impurity below that obtained for the Ni plate.

The results of simulations show that the power load to the plate is lower for Nickel plate than for Carbon for all considered values of the average electron density. This indicates that for low Z materials (carbon) it would be indispensable to use additional impurity in order to reduce power load to the target plates. Additionally for low Z materials (carbon) large impurity concentration is found since the energy flux to the plate is carried mainly by the impurity ions. However, in this case the plasma contamination is low as the result of good impurity screening which is characteristic for the high density tokamaks. It should be noted that for low

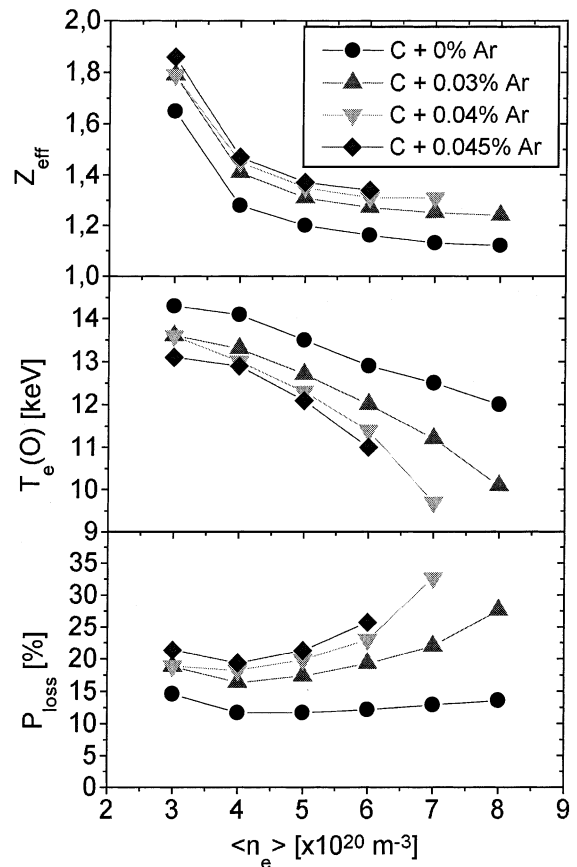


Fig. 4. Z_{eff} , $T_e(O)$ and P_{loss} versus average electron density $\langle n_e \rangle$ for carbon plate with different concentrations of Ar.

Z plate materials the plate erosion might be a very serious problem.

References

- [1] M. Fichtmueller et al., Czechoslovak J. Phys. 48 (1998) 25.
- [2] R. Zagorski, R. Stankiewicz, Czechoslovak J. Phys. 48 (1998) 195.
- [3] B. Coppi, M. Nassi, L.E. Sugiyama, Phys. Scr. 45 (1992) 112.
- [4] J. Mandrekas, J.W.M. Stacey, Nucl. Fus. 35 (1995) 843.
- [5] G. Cenacchi et al., in: Proceedings of the 26th EPS Conference on CFPP, Maastricht, 1999, p. 1121.
- [6] R. Zagorski et al., Nucl. Fus. 36 (1996) 873.
- [7] D.E. Post et al., Atomic Data and Nucl. Data Tables 20 (1977) 397.
- [8] J. Hawryluk et al., Nucl. Fus. 19 (1979) 607.
- [9] P.H. Rutherford, Phys. Fluids 17 (1974) 1782.
- [10] R. Zagorski et al., Phys. Scr. 56 (1997) 399.
- [11] P.C. Stangeby, G.M. McCracken, Nucl. Fus. 30 (7) (1990) 1225.
- [12] R. Zagorski, F. Romanelli, Nucl. Fus. 36 (1996) 853.